Eur. Phys. J. B **41**, 79–85 (2004)
DOI: 10.1140/epjb/e2004-00297-3

THE EUROPEAN PHYSICAL JOURNAL B

Off equilibrium dynamics in the 3d-XY system

S. Abriet and D. Karevski[a]

Laboratoire de Physique des Matériaux, UMR CNRS No. 7556, Université Henri Poincaré (Nancy 1), B.P. 239, 54506 Vandœuvre-lès-Nancy Cedex, France

Received 26 May 2004 / Received in final form 12 July 2004
Published online 30 September 2004 –

Abstract. We investigate through Monte Carlo simulations the non-equilibrium behaviour of the three-dimensional XY-model quenched from a high temperature state to its ferromagnetic and critical phases. The two-times autocorrelation and response functions are determined in the asymptotic (scaling) regime, from which the nonequilibrium exponents λ and critical λ^c are extracted. The form of the scaling function is in agreement with the prediction of local scale-invariance. The so-called limit fluctuation-dissipation ratio X_∞ is shown to vanish in the ordered phase and to reach a constant value around 0.43 for the critical quench.

PACS. 75.40.Gb Dynamic properties – 05.70.Ln Non-equilibrium and irreversible thermodynamics

1 Introduction

After the investigations on aging in glass models [1,2], efforts have been concentrated on the study of non-disordered model systems since it was soon realized that some of the basic aspects of aging are present in simple systems too with some characteristic features [3–5]. In most studies, special attention is put on pure ferromagnetic models undergoing a second order phase transition. Typically, one cools down a sample initially prepared in its high temperature phase to its ordered phase. As time is running, domains start to grow with a linear size $l \sim t^{1/z}$. In the thermodynamic limit, equilibrium is never reached which implies an infinite relaxation time [6]. In order to probe aging, which implies a full dependence on the past evolution, it is useful to compute two-times correlations:

$$C(t,t_w) = \langle \sigma(t)\sigma(t_w)\rangle \tag{1}$$

and linear responses

$$R(t,t_w) = \left.\frac{\delta\langle\sigma(t)\rangle}{\delta h(t_w)}\right|_{h=0} \tag{2}$$

where σ is the order parameter, t the observation time and t_w the waiting time ($\leq t$).
Usually, at a coarse-grained level, the dynamics of such systems is described by a Langevin equation [6]:

$$\frac{\partial\phi_i(t)}{\partial t} = -\frac{\delta H[\phi]}{\delta\phi_i} + \eta_i(t) \tag{3}$$

where H is the free-energy functional, $\eta_i(t)$ is a thermal gaussian noise at site i with:

$$\langle\eta_i(t)\rangle = 0 \quad , \quad \langle\eta_i(t)\eta_j(t')\rangle = 2T\delta(t-t')\delta_{i,j} \; . \tag{4}$$

As mentioned above, the breakdown of time translation invariance implies that the two-time functions do not merely depend on $t-t_w$ but explicitly on t and t_w. On the bases of general scaling arguments, one postulates the following scaling laws for the autocorrelation and autoresponse functions:

$$C(t,t_w) \approx t_w^{-b} f_C(t/t_w) \tag{5}$$

and

$$R(t,t_w) \approx t_w^{-1-a} f_R(t/t_w) \; . \tag{6}$$

In the asymptotic limit, where $t \gg t_w \gg 1$, f_C and f_R decay algebraically:

$$f_C(x) \sim x^{-\lambda_C/z}, \quad f_R(x) \sim x^{-\lambda_R/z} \tag{7}$$

where z is the dynamic exponent and $\lambda_{C,R}$ are respectively the correlation [7] and response exponents [34].

A consequence of the breakdown of time-translation invariance is the violation of the fluctuation-dissipation theorem (FDT) which relates for equilibrium systems the response to the correlation function via:

$$R(t-t_w) = \frac{1}{T}\frac{\partial C(t-t_w)}{\partial t_w} \; . \tag{8}$$

When the system is not at equilibrium $R(t,t_w)$ and $C(t,t_w)$ both depend on t and t_w, and the FDT (8) does not hold anymore. One introduces a new function $X(t,t_w)$ defined by [5]:

$$R(t,t_w) = \frac{X(t,t_w)}{T}\frac{\partial C(t,t_w)}{\partial t_w} \; , \tag{9}$$

[a] e-mail: Karevski@lpm.u-nancy.fr

which measures the deviation from equilibrium. In some mean-field theory of glassy systems, where it was first formulated, the fluctuation-dissipation ratio (FDR) $X(t,t_w)$ depends on time only through a functional dependence on $C(t,t_w)$ [2], that is $X = X(C(t,t_w))$. In this case, integrating (9) with respect to t_w, one gets $T\chi = \int_{C(t,t_w)}^{1} X(C')dC'$, so that the slope of the parametric plot susceptibility χ versus the correlation function C will give the FDR. In the asymptotic regime, for such pure ferromagnetic models, the FDR reaches a constant value X_∞ after an initial quasi-equilibrium regime where $X = 1$ (FDT valid). It was argued that this asymptotic constant is universal and characterises the non-equilibrium process [11]. When a ferromagnetic system is quenched toward its ferromagnetic phase, the long-time dynamics is governed by the diffusion of domain walls and the coarsening of domains. This coarsening leads to a vanishing FDR $X_\infty = 0$ [5,8–10]. The scaling functions defined previously are fullfilling this requirement. In the case of a critical quench, that is exactly at the critical temperature, several studies on various systems have given some insights. In that case, the reason for aging is related to the development of the spatial correlations over a length scale ξ that grows as t^{1/z_c} where z_c is the critical dynamic exponent. So the system is still disordered over a length scale larger than $\xi(t)$, while it looks critical in regions smaller than $\xi(t)$. In the thermodynamic limit, the equilibration is unaccessible since the system is of infinite size so ξ indefinitely increases. For a fully disordered initial state, one has in the kinetic spherical model $X_\infty = 1 - 2/d$ for $2 < d < 4$ and $X_\infty = 1/2$ for $d \geq 4$ [11], in the $1d$ Glauber-Ising model $X_\infty = 1/2$ [11,12]. For algebraic initial correlations, it was shown on the kinetic spherical model that there exists a rich kinetic phase diagram, depending on the space-dimension d and the algebraic decay exponent ω [34], where the limit value X_∞ is either vanishing or depending on d and ω. In the 1d Glauber-Ising model, it was shown that X_∞ is independent on ω [13]. A systematic field-theoretical approach was developed to calculate the limit FDR [14] and applied to several models, ferromagnetic systems at criticality, dilute Ising model, model C dynamics [15–17]. Simulations in $2d$ systems gave $X_\infty = 0.34$ for the Ising model [32,18], $X_\infty = 0.41$ for the three states Potts model, $X_\infty = 0.47$ for the 4-states Potts model [33]. In $3d$, $X_\infty = 0.40$ was obtained for the Ising model [11]. Recently, performing a Monte Carlo simulations with Glauber dynamics, we found from the susceptibility versus correlation function slope a continuously varying FDR in the 2-d XY model quenched below the Kosterlitz-Thouless point [19,20]. But in this case, one has to use with great care this slope, since the actual definition of the FDR X_∞ leads to a logarithmically vanishing result. In this paper, we present the results obtained on the 3-d XY model quenched onto criticality and below.

2 The 3d XY-model

The XY-model is one of the most popular theoretical models. As it is well-known, in the two-dimensional case in the thermodynamical limit there is no finite magnetization at non-zero temperature, but nevertheless there is indeed a topological phase transition occurring at finite temperature due to vortex pairing [21,22]. In three dimensions, the scenario is more conventional since the additional dimension permits the existence of an ordered phase at finite temperature. Thus, the 3d-system presents a second-order phase transition which is probably related to the density of vortex-strings [23,24]. The Hamiltonian reads:

$$\mathcal{H} = -\sum_{\langle i,j \rangle} \boldsymbol{S}_i \cdot \boldsymbol{S}_j \tag{10}$$

where i, j are nearest neighbour sites on a cubic lattice and the $\boldsymbol{S}_i$ are two-dimensional classical spins whose length is set to unity. From high-temperature series analyses, the predicted critical inverse temperature is [25]: $\beta_c = 1/T_c = 0.4539 \pm 0.0013$. In our simulations, we use the value $\beta_c = 1/T_c = 0.4542$ obtained from a Monte Carlo study [26]. The critical exponents have been estimated by renormalisation group techniques and ϵ-expansions [27,28]. In our study we take the values of the critical exponents obtained in reference [29] from a numerical approach:

$$\beta \simeq 0.349 \qquad \nu \simeq 0.672\ . \tag{11}$$

Simulations on the three-dimensional XY model with periodic boundary conditions have revealed that the critical dynamics exponent z_c is close to 2 [30,31]. For a quench below the critical temperature, that is in the ordered phase, one has $z = 2$ [6].

3 Numerics

We simulate the dynamics through a single spin-flip algorithm of Glauber like form where the transition rates p related to the single flip $\{\theta_i\} \to \{\theta_i'\}$, where the θs are the angular variables of the XY model, reads:

$$p(\{\theta_i\} \to \{\theta_i'\}) = \frac{\exp(-\beta\mathcal{H}[\theta_i'])}{\exp(-\beta\mathcal{H}[\theta_i]) + \exp(-\beta\mathcal{H}[\theta_i'])} \tag{12}$$

with β the inverse temperature. One may notice here that the Metropolis algorithm, with transition rate $p = \min[1, \exp(-\beta\Delta E)]$, leads to the same time evolution of the autocorrelation and susceptibilities, as we have checked it.

The two-times autocorrelation function is calculated via

$$C(t,t_w) = \frac{1}{L^3}\sum_i \langle \cos\left[\theta_i(t) - \theta_i(t_w)\right]\rangle \tag{13}$$

where the brackets $\langle \cdot \rangle$ stand for an average over initial configurations and realisations of the thermal noise.

The two-times linear magnetic susceptibility $\chi(t,t_w)$ can be computed by the application of a random magnetic field. The amplitude of the field has to be small in order to

avoid nonlinear effects. The ZFC-susceptibility is usually computed utilising a random distributed field via [8]:

$$\chi(t,t_w) = \frac{1}{h^2 L^3} \sum_i \overline{\langle h_x \cos\theta_i(t) + h_y \sin\theta_i(t)\rangle} \qquad (14)$$

where the line stands for an average over the field realisations. Indeed, here we concentrate on a different approach which is based on the lines of reference [32]. By definition, the linear autoresponse function $R(t,t_w)$ is

$$R(t,t_w) = \frac{1}{L^3} \sum_i \left(\frac{\delta\langle\cos\theta_i(t)\rangle}{\delta h_x(t_w)} + \frac{\delta\langle\sin\theta_i(t)\rangle}{\delta h_y(t_w)} \right)\Big|_{h=0} . \qquad (15)$$

Following reference [32], we can reexpress the linear response function in the form [20]:

$$R(t,t_w) = \beta\langle\cos\theta_i(t)[\cos\theta_i(t_w+1) - \cos\theta_i^w(t_w+1)]\rangle + \beta\langle\sin\theta_i(t)[\sin\theta_i(t_w+1) - \sin\theta_i^w(t_w+1)]\rangle , \qquad (16)$$

where $\cos\theta_i^w$ and $\sin\theta_i^w$ are the components of the local Weiss magnetisation:

$$S_i^{x,y} = \frac{1}{\beta} \frac{\partial}{\partial h_{x,y}} \ln Z_i \Big|_{h=0} , \qquad (17)$$

where $Z_i = \exp(-\beta H(\theta_i, h)) + \exp(-\beta H(\theta_i', h))$ is the local partition function in the field. Finally the fluctuation dissipation ratio is calculated via

$$X(t,t_w) = \frac{TR(t,t_w)}{C(t,t_w+1) - C(t,t_w)} . \qquad (18)$$

4 Results

4.1 Quenches below T_c

We present the results obtained on systems of linear size $L = 50$, with periodic boundary conditions, quenched in the low-temperature phase from an infinite-temperature initial state. The averages are performed with the use of more than 5000 samples. The expected behaviour of the two-times autocorrelation function for coarsening processes is at sufficiently long times [6]:

$$C(t,t_w) = M_{eq}^2(T) f_C\left(\frac{t}{t_w}\right) \qquad (19)$$

where $M_{eq}(T)$ is the equilibrium magnetisation at the temperature T. In order to check this behaviour, we have simulated quenches at two different temperatures, $T = 0.9$ and $T = 1.5$, using the Glauber like dynamics. The results are shown respectively in Figures 1 and 2.

For small time separations, we clearly see that the correlations rapidly decay to the expected plateau values $M_{eq}^2(T)$, here estimated numerically by the use of an independent Wolff algorithm simulation [35,36]. For large time separations, the system enters in a scaling region where

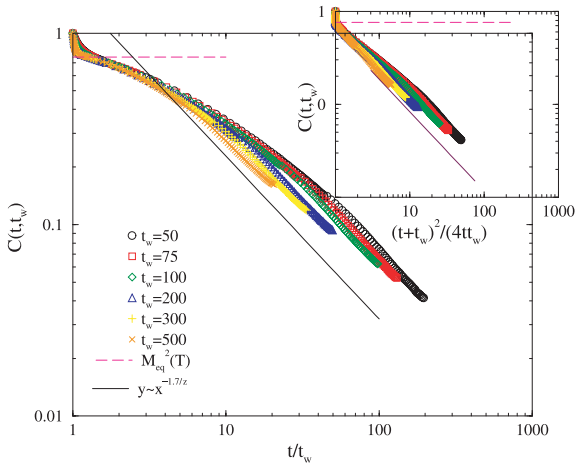

Fig. 1. Asymptotic behaviour of the autocorrelation function at $T = 0.9$. The dashed line corresponds to the value $M_{eq}^2(T)$ and the solid line represents the algebraic decay of $f(t/t_w)$.

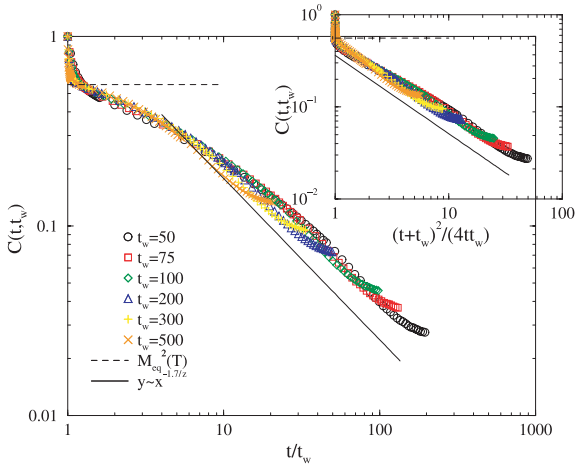

Fig. 2. Asymptotic behaviour of the autocorrelation function at $T = 1.5$. The dashed line corresponds to the value $M_{eq}^2(T)$ and the solid line describes the algebraic decay of $f(t/t_w)$.

the correlation functions are described by a scaling function f_C of the variable $x = t/t_w$. As expected, the aging scaling function finally decays algebraicly in the asymptotic limit with an exponent λ_C roughly about 1.7 ± 0.1. However, we clearly see that as the temperature is increased the finite-size effects become stronger. One may notice also that at smaller temperature one has to wait longer in order to enter in the scaling regime, as it can be seen in Figure 1.

If one accepts the value $\lambda_C = 1.7$, since it is very close to the free field value $\lambda_C^0 = d/2 = 1.5$, one can expect a scaling form of the two-times autocorrelation function not too far from the free-field form [37]:

$$C^0(t,t_w) = M_{eq}^2(T) \left(\frac{(x+1)^2}{4x}\right)^{-\lambda_C^0/2} , \qquad x = t/t_w . \qquad (20)$$

Accordingly, we have replotted in the inset of Figure 1 and Figure 2 the two-times autocorrelation as a function of the

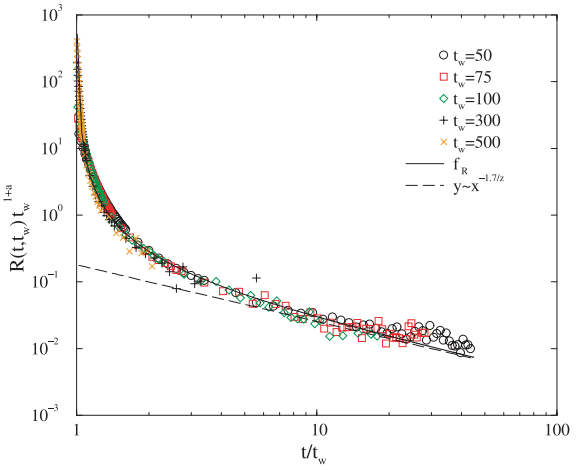

Fig. 3. Scaling behaviour of the response function at $T = 0.9$ for different waiting times. The solid line gives the local-scale invariance prediction with $r_0 = 0.18$. The dashed line is a guide to the eyes for the power law behaviour.

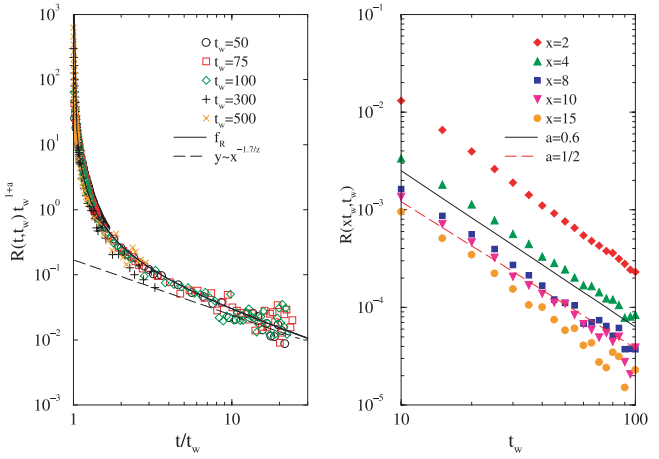

Fig. 4. Left: Scaling behaviour of the response function at $T = 1.5$ for different waiting times. The solid line gives the local-scale invariance prediction with $r_0 = 0.18$. The dashed line is a guide to the eyes for the power law behaviour. Right: Power-law decay of the response function at fixed $x = t/t_w$ ratios and $T = 1.5$. The results are corroborating the value $a = 1/2$.

scaling variable $y = \frac{(x+1)^2}{4x}$. Within this new scaling variable, the power-law form, with $\lambda_C = 1.7$, is remarkable.

In the low-temperature phase, the behaviour of the two-times response function had been conjectured to be (see Ref. [4] for a review):

$$R(t, t_w) \simeq t_w^{-1-a} f_R\left(\frac{t}{t_w}\right) \tag{21}$$

where the scaling function $f_R(x) \approx x^{-\lambda_R/z}$ at $x \gg 1$. Furthermore, if one assumes that the response function transforms covariantly under local scale-transformations, one expects for the scaling function f_R [38,39]

$$f_R(x) = r_0 x^{1+a-\lambda_R/z}(x-1)^{-1-a} \tag{22}$$

where r_0 is a normalization constant. For a disordered initial state we expect [37] $\lambda_R = \lambda_C = \lambda$, with the nonequilibrium exponent λ bounded by [7,40,41]: $d/2 \leq \lambda \leq d$, where d is the Euclidean dimension of the system.

We have computed the autoresponse function at temperatures $T = 0.9$ and $T = 1.5$. In Figure 3 and Figure 4(left), assuming that $a = 1/2$, the rescaled response function is plotted as a function of t/t_w. The collapse of the different waiting time curves is quite good. The value $a = 1/2$ had been already found numerically and analytically in the 3D Glauber-Ising model [39,9] and the 3D kinetic spherical model [34,11]. We have performed an analysis at fixed ratio t/t_w that corroborates the power law prefactor in (21) with a close to 1/2 at large t/t_w as seen in Figure 4. In fact, numerically we obtain a value which is slightly larger than 1/2, around 0.6 but the tendency when increasing t/t_w is toward the decrease of the effective a value. One may notices here that it exists a controversy on the interpretation and value of the exponent a [42,43].

Due to important thermal fluctuations the algebraic regime $x^{-\lambda_R/z}$ is hardly accessible. However, our data

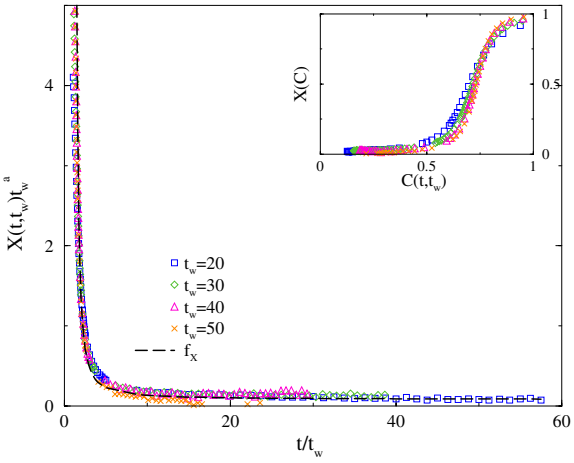

Fig. 5. Rescaled Fluctuation-Dissipation ratio Xt_w^a for a quench in the ferromagnetic phase at $T = 0.9$. The inset is a parametric plot of X versus correlation function.

seem to validate the relation $\lambda_C = \lambda_R$ as it can be seen in Figure 3 and Figure 4 for $T = 0.9$ and $T = 1.5$ respectively. Moreover, as it can be seen from Figures 3 and 4, the scaling form (22) predicted from local scale invariance is perfectly reproduced by our data with $r_0 = 0.18$.

As discussed in the previous section, the asymptotic value of the fluctuation-dissipation ratio X_∞ is expected to vanish in the low temperature phase. Assuming that $\lambda_C = \lambda_R$, the fluctuation-dissipation ratio evaluated from the asymptotic behaviour of (19) and (21) vanishes as:

$$X(t, t_w) \simeq t_w^{-a} f_X(t/t_w) \tag{23}$$

where $f_X(x)$ is a scaling function related to $f_C(x)$ and $f_R(x)$ with $\lim_{x\to\infty} f_X(x) = const.$, a time-independent constant. In Figure 5 we have plotted the rescaled FDR obtained numerically at $T = 0.9$, assuming $a = 1/2$, for

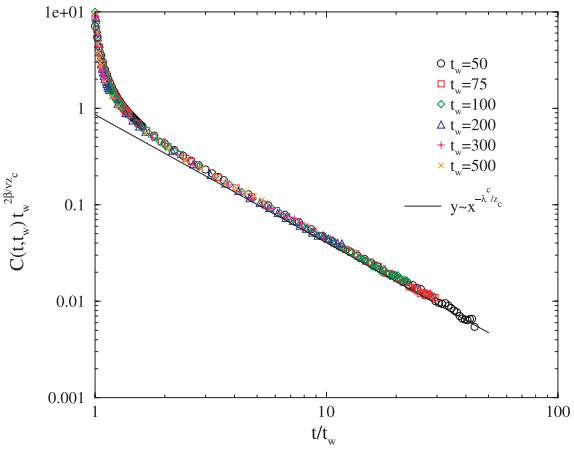

Fig. 6. Rescaled autocorrelation functions for a critical quench of the 3D XY-model. The slope of the solid line stands for $-\lambda_C^c/z_c \simeq -1.34$.

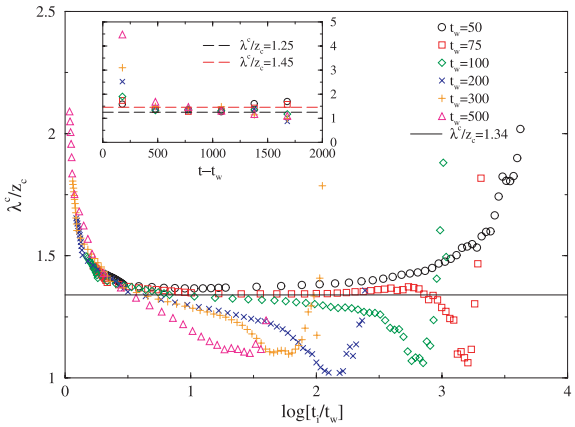

Fig. 7. Effective exponent λ_C^c/z_c for different waiting times at the critical point as a function of t obtained from systems of size $L = 50$.

different waiting times as a function of t/t_w. We see a very good collapse of the different waiting time data. The solid line is the expected scaling form obtained from the definition of the FDR together with the scaling functions f_C and f_R assuming the local scale prediction with $r_0 = 0.18$. Asymptotically, the scaling function f_X reaches a constant value:

$$\lim_{x\to\infty} f_X(x) = \frac{Tr_0}{M_{eq}^2(T)\lambda 2^{\lambda-1}} \tag{24}$$

which is close to 0.08 at $T = 0.9$. In the inset graph of Figure 5, we have represented the FDR $X(t, t_w)$ as a function of the autocorrelation function $C(t, t_w)$ for different waiting times, where we see the vanishing of the X ratio as the correlation decay.

4.2 Critical quench

We focus now on the critical quench starting from a high-temperature initial state. In the vicinity of the critical point, the magnetisation at equilibrium behaves as $|T - T_c|^\beta \sim \xi_{eq}^{-\beta/\nu}$ and with $\xi_{eq} \sim t_w^{1/z_c}$, one expects for the two-times autocorrelation function the form:

$$C(t, t_w) = A_C^c\, t_w^{-2\beta/\nu z_c} f_C^c\left(\frac{t}{t_w}\right) . \tag{25}$$

The expected scaling for the autoresponse function is given by

$$R(t, t_w) = A_R^c\, t_w^{-1-2\beta/\nu z_c} f_R^c\left(\frac{t}{t_w}\right) . \tag{26}$$

The scaling functions $f_{C,R}^c$ are expected to decay algebraicly at large time separation with the same exponent $\lambda_R^c = \lambda_C^c$, however different from the low-temperature one.

The numerical calculations have been performed on periodic cubic lattices of linear size up to $L = 50$ and the physical quantities have been averaged over 5000 noise realisations. In Figure 6 we have plotted the rescaled two-times autocorrelation functions for different waiting times. The collapse of the rescaled functions is very good, in agreement with the form (25). Moreover, at large t/t_w we clearly see a power-law behaviour from which by an algebraic fit we extracted the exponent $\lambda_C^c/z_c \simeq 1.34$ that fulfills the scaling bounds $d/2 \le \lambda_C^c \le d$ (remember that z_c is close to 2). Analysing more carefully the data, we obtain a serie of estimates for the exponent λ_C^c/z_c that are represented in Figure 7. Our final estimate is

$$\lambda_C^c/z^c = 1.34 \pm 0.05. \tag{27}$$

We have also explored the finite-size effects in more details. For that purpose we have studied the time evolution of cubic systems of linear sizes $L = 10, 20, 30$ and 40. Assuming that

$$C(t, t_w, L) = b^{-2\beta/\nu} C(b^{-z_c}t, b^{-z_c}t_w, b^{-1}L) \tag{28}$$

with $b = L$ we obtain the scaling form

$$C(t, t_w, L) = L^{-2\beta/\nu}\mathcal{F}\left(\frac{t}{L^{z_c}}, \frac{t_w}{L^{z_c}}\right) . \tag{29}$$

In Figure 8, we have plotted $\mathcal{F}$ for different sizes at fixed ratio $x \equiv t_w/L^{z_c} = 0.1$ as a function of t/L^{z_c}. Taking into account (25) and (29), we expect that the scaling function $\mathcal{F}$ has an algebraic decay with the exponent $-\lambda_C^c/z_c$ for t not too large. The collapse of the curves is quite good. For earliest times the system is still in quasi-equilibrium and for biggest times the growth of correlated domains is limited by the size of the system. The numerical data seem to validate the scaling assumption (29).

We focus now on the autoresponse functions computed with formula (16). The quantities are quite noisy since thermal fluctuations are of the same order as the amplitude of the response at long times. From (6), one should have $a = b$ and $\lambda_R^c = \lambda_C^c = \lambda^c$ since the initial state is fully disordered. In Figure 9, the rescaled autoresponse is represented as a function of t/t_w for several waiting

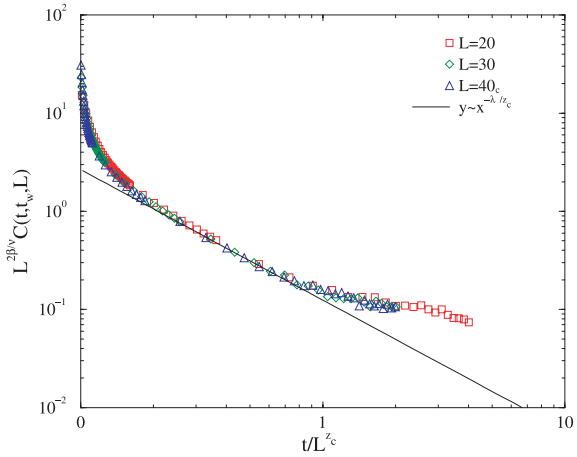

Fig. 8. Rescaled autocorrelation functions for different system sizes at the critical point. All the curves collapse in the full-aging regime where the scaling function F decays as $(t/L^{z_c})^{\lambda_C^c/z_c}$

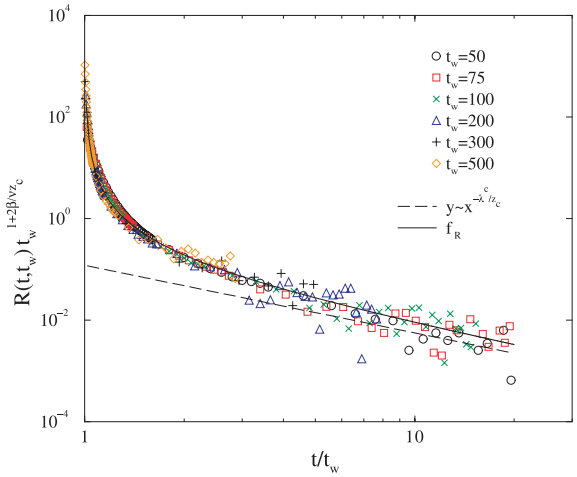

Fig. 9. Rescaled autoresponses as a function of t/t_w for different waiting times and for a critical quench. The solid line gives the scaling function as predicted by local scale invariance. The dashed line gives the algebraic decay $(t/t_w)^{-\lambda_R^c/z_c}$ with $\lambda_R^c/z_c = \lambda_C^c/z_c = 1.34$.

times t_w. We see that the decay of the autoresponse function is compatible with the algebraic assumption with $\lambda_R^c/z_c = \lambda^c/z_c \simeq 1.34$.

As stated previously, the out-of equilibrium behaviour is somehow characterised by the FDR $X(t,t_w)$, calculated numerically via (18). Assuming the scaling forms of the two-times autocorrelation and response functions, the FDR is supposed to be a function of the ratio t/t_w only. This behaviour is well reproduced in Figure 10, where we have plotted the FDR $X(t,t_w)$ as a function of t_w/t calculated on a system of linear size $L = 30$, and for different waiting times. In the long time limit $t_w/t \to 0$, the FDR approaches a constant value, around 0.4, but due to the numerical noise, basically related to the numerical derivative of $C(t,t_w)$, it is difficult to give a more precise value.

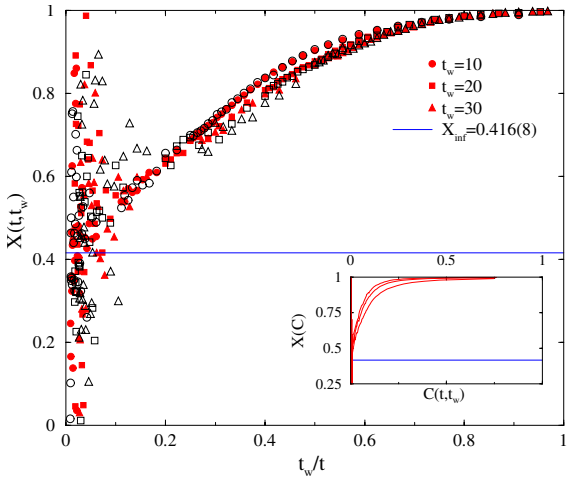

Fig. 10. Fluctuation Dissipation ratio at the critical point as a function of t_w/t for $L = 20$ (open symbols) and $L = 30$ (filled symbols). The solid line gives the analytical result $X_\infty = 0.416(8)$ of reference [15]. The inset shows the dependence of X with the same waiting times as a function of the correlation C.

However, if one supposes an asymptotic linear form

$$X(t,t_w) \simeq X_\infty + \delta \frac{t_w}{t} \,, \tag{30}$$

it is possible to extract the value:

$$X_\infty = 0.43 \pm 0.04 \,. \tag{31}$$

In reference [15], the limit FDR was calculated in an ϵ expansion. The two-loop expansion leads to a value $X_\infty = 0.416(8)$ that perfectly fits, within the error bars, our estimate.

5 Conclusion and outlooks

We have studied the relaxation behaviour of the 3D XY-model quenched from its high temperature state to its ferromagnetic phase and at criticality. Through Monte Carlo simulations, we have computed the autocorrelation function and its conjugate response function on cubic lattices of maximal linear size $L = 50$. From our data, we have confirmed the general scaling scenario at and below criticality. The autocorrelation non-equilibrium exponent λ_C below T_c was found to be around 1.7. The scaling analysis of the linear autoresponse function confirmed the equality $\lambda_R = \lambda_C = \lambda$, expected for quenches from a fully disordered initial state. At criticality, we have confirmed that the correlation and response function behave as: $C(t,t_w) = t_w^{-b} f_C^c(t/t_w)$ and $R(t,t_w) \approx t_w^{-1-a} f_R^c(t/t_w)$, with $a = b = 2\beta/\nu z_c$. This conclusion has been supported by a finite-size analysis on systems of linear sizes $L = 10, 20, 30, 40$ and 50. From the data on the correlation function we extracted the value $\lambda^c/z_c \simeq 1.34$ for the nonequilibrium critical exponent and checked its compatibility with the response function data. One may notice that this value is very close to that obtained in the

$3d$-Ising model, that is $\lambda^c \simeq 2.8$ [7]. It is remarkable to notice that the local scale-invariance prediction for the response function is very nicely fulfilled either at criticality and below. Although at criticality field-theoretical approach [14] showed a deviation from the local scale invariance prediction [15], it is very difficult to see numerically this very small discrepancy. In the ordered phase, since the nonequilibrium exponent is very close to the free-field value $d/2$, we have shown that the autocorrelation function has a scaling form which is very close to that of the free-field: $C(t,t_w) = M_{eq}^2 y^{-\lambda/z}$ with the scaling variable $y = (x+1)^2/(4x)$ where $x = t/t_w$. The direct calculation of the FDR $X(t,t_w)$ showed that, as expected, in the low temperature phase it vanishes like $X_\infty(t,t_w) = t_w^{-a} f_X(t/t_w)$ where f_X is a scaling function simply related to the local scale-invariance scaling functions f_C and f_R. The same analysis at the critical point gave a limit FDR $X_\infty = 0.43$, which is in agreement, within the error bars, with the field theoretical value obtained in reference [15] To conclude, we have studied the $3d - XY$ model in the context of aging and showed that the results obtained are consistent with the general picture usually drawn. Moreover, we have given a new verification of the local scale-invariance predictions, the first for a non-scalar order parameter.

We wish to thank C. Chatelain and M. Henkel for useful discussions and critical reading of the paper. P. Calabrese and A. Gambassi are greatfully acknowledged for helpful comments.

References

1. J.-P. Bouchaud, L.F. Cugliandolo, J. Kurchan, M. Mézard, in *Spin Glasses and Random Fields*, edited by A.P. Young (World Scientific, Singapore, 1998); L.F. Cugliandolo, Lecture notes, Les Houches, July 2002, `cond-mat/0210312`
2. L.F. Cugliandolo, J. Kurchan, J. Phys. A **27**, 5749 (1994)
3. L.F. Cugliandolo, J. Kurchan, L. Peliti, Phys. Rev. E **55**, 3898 (1997)
4. C. Godreche, J.M. Luck, J. Phys.: Condens. Matter **14**, 1589 (2002); M. Henkel, Adv. Solid State Phys. **44** (2004), in press (`cond-mat/0404016`)
5. L.F. Cugliandolo, J. Kurchan, G. Parisi, J. Phys. I France **4**, 1641 (1994)
6. A.J. Bray, Adv. Phys. **43**, 357 (1994)
7. D.S. Fisher, D.A. Huse, Phys. Rev. B **38**, 373 (1988); D.A. Huse, Phys. Rev. B **40**, 304 (1989)
8. A. Barrat, Phys. Rev. E **57**, 3629 (1998)
9. L. Berthier, J.L. Barrat, J. Kurchan, Eur. Phys. J. B **11**, 635 (1999)
10. S.A. Cannas, D.A. Stariolo, F.A. Tamarit, Physica A **294**, 362 (2001)
11. C. Godreche, J.M. Luck, J. Phys. A **33**, 9141 (2000)
12. E. Lippiello, M. Zannetti, `cond-mat/0001103`
13. M. Henkel, G.M. Schütz, J. Phys. A **37**, 591 (2004)
14. P. Calabrese, A. Gambassi, Phys. Rev. E **65**, 066120 (2002)
15. P. Calabrese, A. Gambassi, Phys. Rev. E **66**, 066101 (2002)
16. P. Calabrese, A. Gambassi, Phys. Rev. B **66**, 212407 (2002)
17. P. Calabrese, A. Gambassi, Phys. Rev. E **67**, 036111 (2003)
18. P. Mayer, L. Berthier, J. Garrahan, P. Sollich, Phys. Rev. E **68**, 016116 (2003)
19. Berthier, Holdsworth, Sellitto, J. Phys. A **34**, 1805 (2001)
20. S. Abriet, D. Karevski, Eur. Phys. J. B **37**, 47 (2004)
21. V.L. Berezinskii, Sov. Phys. JETP **32**, 493 (1971)
22. J.M. Kosterlitz, D.J. Thouless, J. Phys. C **6**, 1181 (1973); J.M. Kosterlitz, J. Phys. C **7**, 1046 (1974); J. Villain, J. Phys. France **36**, 581 (1975)
23. G. Kohring, R.E. Shrock, P. Wills, Phys. Rev. Lett. **57**, 1358 (1986)
24. G.A. Williams, Phys. Rev. Lett. **59**, 1926 (1987)
25. M. Ferer, M.A. Moore, M. Wortis, Phys. Rev. B **8**, 5205 (1973)
26. A.P. Gottlob, M. Hasenbusch, Physica A **201**, 593 (1993)
27. J.C. Le Guillou, J. Zinn-Justin, Phys. Rev. B **21**, 3976 (1980); R. Guida, J. Zinn-Justin, J. Phys. A **31**, 8103 (1998)
28. K.G. Wilson, M.E. Fisher, Phys. Rev. Lett. **28**, 240 (1972)
29. M. Hasenbusch, T. Török, J. Phys. A **32**, 6361 (1999)
30. L.M. Jensen, B.J. Kim, P. Minnhagen, Europhys. Lett. **49**, 644 (2000); P. Minnhagen, B.J. Kim, H. Weber, Phys. Rev. Lett. **87**, 037002 (2001)
31. M. Mondello, N. Goldenfeld, Phys. Rev. A **42**, 5865 (1990); M. Mondello, N. Goldenfeld, Phys. Rev. A **45**, 657 (1992)
32. C. Chatelain, J. Phys. A **36**, 10739 (2003); F. Ricci-Tersenghi, Phys. Rev. E **68**, 065104(R) (2003)
33. C. Chatelain, J. Stat. Mech.: Theor. Exp. P06006 (2004)
34. A. Picone, M. Henkel, J. Phys. A **35**, 5575 (2002)
35. U. Wolff, Phys. Rev. Lett. **62**, 361 (1989)
36. W. Janke, Phys. Lett. A **148**, 306 (1990)
37. A. Picone, M. Henkel, Nucl. Phys. B **688**, 217 (2004)
38. M. Henkel, Nucl. Phys. B **641**, 405 (2002)
39. M. Henkel, M. Pleimling, C. Godrèche, J.-M. Luck, Phys. Rev. Lett. **87**, 265701 (2001)
40. T.J. Newman, A.J. Bray, J. Phys. A **23**, 4491 (1990); J.G. Kissner, A.J. Bray, J. Phys. A **26**, 1571 (1993)
41. C. Yeung, M. Rao, R.C. Desai, Phys. Rev. E **53**, 3073 (1996)
42. M. Henkel, M. Paessens, M. Pleimling, Europhys. Lett. **62**, 664 (2003)
43. F. Corberi, E. Lippiello, M. Zannetti, C. Castellano `cond-mat/0311046`